JAERI - M
90-187

STUDY ON FUEL DEFORMATION DURING PCIOMR

October 1990

Kazuaki YANAGISAWA and Chen DIANSHAN*

日 本 原 子 力 研 究 所
Japan Atomic Energy Research Institute

JAERI-Mレポートは，日本原子力研究所が不定期に公刊している研究報告書です。
入手の問合わせは，日本原子力研究所技術情報部情報資料課（〒319-11茨城県那珂郡東海村）あて，お申しこしください。なお，このほかに財団法人原子力弘済会資料センター（〒319-11 茨城県那珂郡東海村日本原子力研究所内）で複写による実費頒布をおこなっております。

JAERI-M reports are issued irregularly.
Inquiries about availability of the reports should be addressed to Information Division, Department of Technical Information, Japan Atomic Energy Research Institute, Tokai-mura, Naka-gun, Ibaraki-ken 319-11, Japan.

編集兼発行　日本原子力研究所
印　　刷　㈱原子力資料サービス

Study on Fuel Deformation during PCIOMR

Kazuaki YANAGISAWA and Chen DIANSHAN*

Department of Fuel Safety Research
Tokai Research Establishment
Japan Atomic Energy Research Institute
Tokai-mura, Naka-gun, Ibaraki-ken

(Received September 28, 1990)

In majority of Japanese commercial power reactors, PCIOMR (Pre-Conditioning Interim Operating Management Recommendation) has been utilized widely. This principally aims at reduing the magnitude of pellet-cladding mechanical interaction (PCMI) to be caused in the LWR fuel rod during power rise.

By using open litaratures, the effect of power rise rate on PCMI was evaluated by the Authors. The evaluation was addressed mainly to use data obtained from in-core instrumentations of rod diameter gauge and axial elongation sensor. This kind of evaluation is new.

Obtained results are:

(1) It is revealed from this study that the magnitude of PCMI occurred during PCIOMR (power rise rate of 0.2 kW/m) is about one-half of that occurred during fast power rise rate of 8 kW/m. The principal mechanism dominating this is fuel creep. It affects greatly to reduce the magnitude of ridging at pellet-to-pellet interface location.

(2) Correlation between integrated axial strain and averaged diametral strain at the same power level is important, especially from fuel modelling point of view. However, there was no litarature mentiond about this. From present work, it was found that they

---

* Department of Reactor Engineering Technology, Chinese Institute of Atomic Energy

have not similar magnitude during PCIOMR at beginning-of-life. The former is greater of order of 60% than the latter. However, they tended to have same magnitude with increasing burn-up.

Keywords: Fuel Behavior, PCMI, PCIOMR, Axial Strain, Radial Strain, Fuel Creep

PCIOMR中の燃料ふるまいに関する研究

日本原子力研究所東海研究所燃料安全工学部
柳澤　和章・陳　　殿山*

（1990年9月28日受理）

我が国の大多数の商用炉においては，PCIOMR運転方式が広く導入されている。この運転方式は，出力上昇過程にある軽水炉燃料に生じるとされているペレット－被覆管間の機械的相互作用（PCMI）を減少させることが，主たる目的である。

報告書らは，公開文献に基づいて，この出力上昇速度が燃料のPCMIに与える影響について評価を実施した。ここでは，文献ごとにバラバラに評価された燃料棒の外径変化や長手方向の伸びをPCMIと結びつけ，統一的に行ったものであり，得られた結果は新しい知見を含んでいる。

(1) 本研究から，PCIOMR運転（出力上昇速度0.2 kW／mh）中に発生したPCMIは，高速出力上昇運転（出力上昇速度8 kW／mh）中に発生したPCMIに比較して，約半分である事が明らかになった。このPCMIの著しい低減の主たるメカニズムは，燃料クリープである事も明らかになった。このクリープは，燃料ペレットとペレットの境界面においてPCMI時に発生するリッジングを十分抑制することがわかった。

(2) 燃料のモデリングの観点からは，燃料棒の長手方向軸歪量と直径方向の平均歪量の相関は重要である。しかしながら，この点に関して明確な結論を下した文献はこれまでにみられなかった。本報は，それに着目した研究を行った。その結果，照射初期では両者の歪レベルに相違がある事が明らかになった。すなわち，前者は後者よりも約60%大きかった。しかしながら，燃焼度が増加すると，両者は徐々にほぼ同じ歪レベルに到達する事も明らかになった。

東海研究所：〒319－11 茨城県那珂郡東海村白方字白根2－4
*中国原子能科学研究院　反応堆工程技術研究所

Contents

目　　次

1. INTRODUCTION

An empirical fact in commercial LWR power plants has been led us that the well-controlled operational scheme could minimize the local power variations accompanying with very low propensity for PCI(Pellet Cladding Interaction) failure. This operational manner, however, arises many shortcomings for existing LWRs. For example, PCIOMR (Pre-Conditioning Interim Operating Management Recommendation) which has been adopted widely in LWR power plants[1], will yield the reduction of its availability of order of a few percent per year. This may not be negligible.

PCIOMR is considered to be a very time consuming method for the increase of reactor power because it strongly depends upon time-dependent variables such as power history and burn-ups. For example, in BWR case, the following rate proposed by GE[2] has been recommended as a maximum permissible rate for making the initial PCIOMR envelopment:

$$C_{rm} = 0.33 \left\{ \frac{12.45}{D_n} \right\}^3 \cdot \frac{T_n}{0.81} \quad \cdots\cdots\cdots\cdots /1/$$

in which C_{rm} (kW/mh) is the maximum permissible rate for pre-conditioning as a function of initial peak power and burn-ups, D_n (mm) the as-built diameter of the used UO_2 pellet, and T_n [mm] the thickness of zircaloy-2 cladding.

As to the case for PWRs, the C_{rm} value of 3 $\%h^{-1}$ instead of 0.33 (kW/mh) in equation /1/ has been used[3] as a function of initial peak power and burn-ups.

To overcome these shortcomings and to establish more effective way to reactor start-up, well-characterized data related to PCIOMR have been called for. Adding to this, the reason why PCIOMR is effective to reduce PCI failure is still remained unclear from mechanistic point of view. The mechanism dominating the pellet cladding mechanical interaction (PCMI) during PCIOMR, therefore, should be investigated further. Results may be useful for developing a fuel performance computer code.

The followings are of principal objectives for the present work.

(i) To find out possible mechanism which can reduce the magnitude of PCMI during PCIOMR. This will be addressed not only to first power rise but also to progressed burn-up stages.

(ii) From code modelling point of view, it is strongly necessary to know the relationship between magnitude of an integreted axial strain and that of rod averaged diametral strain. Because almost was modelled in the axial integrated strain only.

In order to accomplish the subjects, open literatures[4-6] were utilized and made detailed data evaluation. They are from experiments performed in Halden Boiling Water Reactor (HBWR), Norway. One was from General Electric (hereinafter called PCIOMR-I experiment)[4] and the other from Japanese vendors under cooperation with JAERI(hereinafter called PCIOMR-II experiment)[5-6], respectively.

This kind of work , however, was not done in previous litaratures. Hence, the results obtained here are new.

2. TEST DESCRIPTION

2.1 Fuel rod characterization

In PCIOMR-I experiment, an influence of power rise rate on PCMI at beginning of life (BOL) was studied. They used two power rise rates as variable, that is, 8 kW/mh and 0.2 kW/mh. Responses were cladding diameter and integrated clad axial elongation. As-built attributes used are shown in Table 1. Used fuels were typical 8x8 BWR type ones.

In PCIOMR-II experiment, an influence of power rise rate as well as diametral gap on PCMI was studied. Here, an influence of burn-up on PCIOMR was also studied. Used power rise rates as variable were 0.2 and 0.7 kW/mh. This was combined with fast power rise of 8 kW/mh. As-built diametral gaps as variable were 0.04 mm and 0.21 mm. Responses were cladding diameter and integrated cladding axial elongation. As-built attributes used are shown in Table 2. Used fuels were typical 8x8 BWR type ones.

Burn-up in this was, however, 1 GWd/tU which was too small to know the burn-up effect well. To compensate this, we further looked for the BWR data and obtained from JAERI experiment at HBWR, where typical BWR type fuel having diameteral gap by 0.1 mm had PCIOMR at 14 GWd/tU. As responses, cladding diameter and integrated cladding axial elongation were used. Detail characteristics of this is described elsewhere[7].

2.2 Evaluation of data

Regarding the method for data evaluation, unforthnately there was no good consistency among the pitaratures. So, reassessment was made to all those by using the following relationships.

(i) Assembly power : QA (kw)

$$QA = k_g \times ND \times C_d(BU) \cdots\cdots\cdots\cdots\cdots\cdots\cdots\cdots\cdots\cdots /2/$$

In order to accomplish the subjects, open literatures[4-6] were utilized and made detailed data evaluation. They are from experiments performed in Halden Boiling Water Reactor (HBWR), Norway. One was from General Electric (hereinafter called PCIOMR-I experiment)[4] and the other from Japanese vendors under cooperation with JAERI(hereinafter called PCIOMR-II experiment)[5-6], respectively.

This kind of work , however, was not done in previous litaratures. Hence, the results obtained here are new.

2. TEST DESCRIPTION

2.1 Fuel rod characterization

In PCIOMR-I experiment, an influence of power rise rate on PCMI at beginning of life (BOL) was studied. They used two power rise rates as variable, that is, 8 kW/mh and 0.2 kW/mh. Responses were cladding diameter and integrated clad axial elongation. As-built attributes used are shown in Table 1. Used fuels were typical 8x8 BWR type ones.

In PCIOMR-II experiment, an influence of power rise rate as well as diametral gap on PCMI was studied. Here, an influence of burn-up on PCIOMR was also studied. Used power rise rates as variable were 0.2 and 0.7 kW/mh. This was combined with fast power rise of 8 kW/mh. As-built diametral gaps as variable were 0.04 mm and 0.21 mm. Responses were cladding diameter and integrated cladding axial elongation. As-built attributes used are shown in Table 2. Used fuels were typical 8x8 BWR type ones.

Burn-up in this was, however, 1 GWd/tU which was too small to know the burn-up effect well. To compensate this, we further looked for the BWR data and obtained from JAERI experiment at HBWR, where typical BWR type fuel having diameteral gap by 0.1 mm had PCIOMR at 14 GWd/tU. As responses, cladding diameter and integrated cladding axial elongation were used. Detail characteristics of this is described elsewhere[7].

2.2 Evaluation of data

Regarding the method for data evaluation, unforthnately there was no good consistency among the pitaratures. So, reassessment was made to all those by using the following relationships.

(i) Assembly power : QA (kw)

$$QA = k_g \times ND \times C_d(BU) \cdots\cdots\cdots\cdots\cdots\cdots\cdots\cdots\cdots\cdots /2/$$

in which k_g (TW/A) is power conversion factor, ND (nA) the averaged neutron value taking rod axial flux change into consideration, and C_d the depletion factor as a function of burn-up.

(ii) Rod local power : P (kW/m)

$$P = k_g \times C_d \times N(i) / L_f \times N \quad \cdots\cdots/3/$$

in which N(i) (nA) is the rod averaged neutron value taking radial and axial distribution of flux, L_f (m) the active fuel column length, and N the total number of rods loaded.

(iii) Burn-up : BU (GWd/tU)

$$BU = \int QA \cdot dt/W = k_g \cdot C_d \int ND \cdot dt/W \quad \cdots\cdots/4/$$

in which W (tU) is the initial loaded fuel weight. Fuel depletion effect on burn-up was accounted for. The accuracy for burn-up by means of in-pile signals from neutron detector was within plus minous 20 %.

(iv) Dimensional conversion

Axial integrated elongation ε_z(%) was converted into axial strain by the following.

$$\varepsilon_z = \frac{\text{Elongation signal from fuel rod (nA)}}{\text{Calibration factor (nA/mm)}} \cdot \frac{100}{L_f(\text{mm})} \quad \cdots/5/$$

Diametral strain ε_h(%) was determined as follows.

$$\varepsilon_h = \sum_{i=1}^{h} (D(i)-D_0)/n \cdot D_0 \times 100 \quad \cdots\cdots/6/$$

in which n is the numbers of ridging observed along fuel rod, D_0 the averaged fuel diameter in hot stand-by condition, and D(i) the fuel diameter at selected axial location i.

Because diameter measurement usually initiated from hot stand-by condition (zero power with coolant temperature 240℃ and coolant pressure 3.4 MPa), relationship between rod cold diameter D(mm: as-built diameter) and rod hot diameter D_0(mm: diameter in stand-by condition) is necessary. We assumed this by

$$D_0 = 1.001531 \times D \quad \cdots\cdots/7/$$

We used this D_0 as zero power diameter. After occurrence of PCMI, we denoted rod diameter as follows: One was the diameter at pellet-to-pellet interface location and the other was the diameterat mid-pellet location. They are abbreviated as D_r, and D_t, respectively.

3. RESULTS

3.1 PCIOMR-I experiment

Figure 1 shows test scheme for PCIOMR-I experiment in which different power rise rate (8kW/mh and 0.2kW/mh) were used for each different BWR fuel rods.

Results of data reassessment are summarized in Table 3. Figures 2 and 3 are the plotting of the table. In the former, axial integrated strains at two different power rise rates are comparing. In the latter, an integrated axial strain (ε_z) during fast power rise and averaged diametral strain (ε_h) during slow power rise are compared. It can be revealed from these that PCIOMR is much effective to reduce the magnitude of PCMI. For example, axial strain and diametral strain under PCIOMR (0.2 kW/mh) is of order of approximately 50 % smaller than those under fast power rise (8 kW/mh).

The fuel deformation during PCIOMR was found to be elastic because there was little residual strain after power removal. On the other hand, the fuel deformation during fast power rise was plastic because the fuel rod had residual strain with magnitude of 0.02 % in diametral and of 0.07 % in axial directions. This diffenece might be attributed to the different magnitude of fuel relaxation (fuel creep) induced by PCIOMR.

Relationship between axial integrated strain and diametral one at representative power level is compared. This kind of comparison is necessary for computer code having only the model of axial strain. Figure 4 shows the result. For fuel rod having power rise rate of 8 kW/mh, a tendency $\varepsilon_z > \varepsilon_h$ is seen. Similar trend is appeared in fuel rod power rised at 0.2 kW/mh. Hence, The magnitude of diametral strain is not equal to that of axial strain at beginning-of-life (BOL). Further, it is worthy mentioning that the magnitude of PCMI in slow power rise was less than that in fast power rise.

The reason why the diametral PCMI during PCIOMR is smaller than axial one is studied. For this, ridge height and diametral strain were plotted from Table 3. Please note that the former has greater stress concentration at pellet-to-pellet interface location. The latter is representing the averaged diametral deformation including the ridging.

Result is shown in Figure 5. During power rise of 8 kW/mh, ridge height and diametral strain increased monotonously with in-

We used this D_0 as zero power diameter. After occurrence of PCMI, we denoted rod diameter as follows: One was the diameter at pellet-to-pellet interface location and the other was the diameterat mid-pellet location. They are abbreviated as D_r, and D_t, respectively.

3. RESULTS

3.1 PCIOMR-I experiment

Figure 1 shows test scheme for PCIOMR-I experiment in which different power rise rate (8kW/mh and 0.2kW/mh) were used for each different BWR fuel rods.

Results of data reassessment are summarized in Table 3. Figures 2 and 3 are the plotting of the table. In the former, axial integrated strains at two different power rise rates are comparing. In the latter, an integrated axial strain (ε_z) during fast power rise and averaged diametral strain (ε_h) during slow power rise are compared. It can be revealed from these that PCIOMR is much effective to reduce the magnitude of PCMI. For example, axial strain and diametral strain under PCIOMR (0.2 kW/mh) is of order of approximately 50 % smaller than those under fast power rise (8 kW/mh).

The fuel deformation during PCIOMR was found to be elastic because there was little residual strain after power removal. On the other hand, the fuel deformation during fast power rise was plastic because the fuel rod had residual strain with magnitude of 0.02 % in diametral and of 0.07 % in axial directions. This diffenece might be attributed to the different magnitude of fuel relaxation (fuel creep) induced by PCIOMR.

Relationship between axial integrated strain and diametral one at representative power level is compared. This kind of comparison is necessary for computer code having only the model of axial strain. Figure 4 shows the result. For fuel rod having power rise rate of 8 kW/mh, a tendency $\varepsilon_z > \varepsilon_h$ is seen. Similar trend is appeared in fuel rod power rised at 0.2 kW/mh. Hence, The magnitude of diametral strain is not equal to that of axial strain at beginning-of-life (BOL). Further, it is worthy mentioning that the magnitude of PCMI in slow power rise was less than that in fast power rise.

The reason why the diametral PCMI during PCIOMR is smaller than axial one is studied. For this, ridge height and diametral strain were plotted from Table 3. Please note that the former has greater stress concentration at pellet-to-pellet interface location. The latter is representing the averaged diametral deformation including the ridging.

Result is shown in Figure 5. During power rise of 8 kW/mh, ridge height and diametral strain increased monotonously with in-

creasing power. On the other hand, it increased little during power rise of 0.2 kW/mh nevertheless the diameteral strain still increased gradually. This behavior might be attributed to significant fuel creep at pellet-to-pellet interface location.

Figure 6 shows the ridge height obtained from slow and fast power rise. Each was plotted against representative power levels. Magnitude of ridge height in the former is almost one-half of that in the latter. Thus, PCIOMR is repeatedly effective to reduce the magnitude of ridging.

3.2 PCIOMR-II experiment

Here, the fuel behavior under PCIOMR with varying as-built diametral gap and burn-up was studied. Power history is schematically shown in Figure 7. This is a partially different from previous experiment because tested rod had two different kinds of power rise rates in a time. It should be noted that this resembled much to conventional PCIOMR used widely in Japanese BWR commercial power plants. Power rise rate in this study was shifted usually from 30 kW/m. This is indicated by the arrow in subsequent figures. Ridge height, averaged diametral deformation and axial elngation data were of major concern. Numerical data obtanied from the reassessment are summarized in Table 4. Basing on this, the following observations are made.

3.2.1 PCMI

Figure 8 shows axial and diametral strain of 0.21 mm gap rod (top two) and that of 0.06 mm gap rod (bottom two). They are given as a function of rod power. In this case, power rise rate was changed from 8 kW/mh to 0.7 kW/mh. Large gap rod represents a typical fuel rod used in commercial BWR power plants. Small gap rod is for comparison.

This shows that the large gap rod at BOL caused little PCMI. While, small gap rod caused greater PCMI. It is worthy mentioning that a magnitude of PCMI between axial direction and diametral one is significantly different. Hence, cladding axial strain after 0.7 kW/mh decreased monotoneously but diametral strain increased gradually with increasing power. This difference might be attributed to different fuel properties like fuel densification stability. Details, however, have not been clarified.

3.2.2 Correlation between axial and diametral PCMI

Figure 9 shows the comparison between axial strain and diametral one. The followings are observed from the figure.

(i) Up to the power of 30 kW/m (power rise rate of 8 kW/mh), a magnitude of axial strain is greater than that of diametral one. That is,

$$\varepsilon_h < \varepsilon_z \quad \cdots\cdots /8/$$

In this case, the magnitude of axial strain was of order of 40 to 60% greater than that of diametral strain depending on initial gap.

(ii) When power rise rate was changed from 8 kW/mh to 0.2-0.7 kW/mh, the relative magnitude of axial strain was decreased gradually with increasing power. Finally, at 40 kW/m, we obtain

$$\varepsilon_h > \varepsilon_z \quad \cdots\cdots/9/$$

Residual strain was different between the two.

Ridge height Dr as a function of hoop strain is shown in Fig. 10. As to the case for 0.04 mm gap rod, ridging of order of approximately 7 μm was initially existed from the hot stand-by condition. It is noticeable that diametral strain increases with increasing power but ridge height does not increase after slow ramp of 0.2 kW/mh. Thus, this type of PCIOMR is also effective to reduce the magnitude of ridging, especially at higher power level.

4. DISCUSSIONS

To find out the effectiveness of PCIOMR at progressed burn-up is important. For, in many commercial power reactors PCIOMR is imposing repeatedly at every certain burn-up levels. This is due to make further new envelope against PCMI.

4.1 PCIOMR at 1 GWd/tU

In previous section 3.2, we revealed that the conventional BWR fuel having a diamtral gap by 0.21 mm caused little PCMI during first rise to maximum power. If one continued the irradiation, a diametral gap will be decreased due mainly to the fuel relocation and the swelling. Hence, higher the burn-up, smaller the rod diametral gap. This gap closure will tend to cause the greater PCMI.

Influence of burn-up on PCIOMR is studied by the fuel rod I-3 shown in Table 2. This was irradiated continuously in the course of PCIOMR-II experiments. Power history of this rod is shown in Fig. 11. As seen from the figure, this had PCIOMR (0.2 kW/mh) during first rise to maximum power and scrummed immediately after reaching 40 kW/m. At approximate burn-up of 1 GWd/tU , this had PCIOMR (0.4 kW/mh) repeatedly.

Result of our reassessment is shown in Figure 12. The followings are obtained :

(1) The magnitude of axial maximum strain at 1 GWd/tU denoted as −●− is smaller of order 40 % than that at start-up (denoted as −○−). At burn-up of 1 GWd/tU, the magnitudes of axial and diametral deformations become relatively smaller than at zero burn-up. There is nearly one to one correspondence between axial strain

In this case, the magnitude of axial strain was of order of 40 to 60% greater than that of diametral strain depending on initial gap.

(ii) When power rise rate was changed from 8 kW/mh to 0.2-0.7 kW/mh, the relative magnitude of axial strain was decreased gradually with increasing power. Finally, at 40 kW/m, we obtain

$$\varepsilon_h > \varepsilon_z \quad \cdots\cdots/9/$$

Residual strain was different between the two.

Ridge height Dr as a function of hoop strain is shown in Fig. 10. As to the case for 0.04 mm gap rod, ridging of order of approximately 7 μm was initially existed from the hot stand-by condition. It is noticeable that diametral strain increases with increasing power but ridge height does not increase after slow ramp of 0.2 kW/mh. Thus, this type of PCIOMR is also effective to reduce the magnitude of ridging, especially at higher power level.

4. DISCUSSIONS

To find out the effectiveness of PCIOMR at progressed burn-up is important. For, in many commercial power reactors PCIOMR is imposing repeatedly at every certain burn-up levels. This is due to make further new envelope against PCMI.

4.1 PCIOMR at 1 GWd/tU

In previous section 3.2, we revealed that the conventional BWR fuel having a diamtral gap by 0.21 mm caused little PCMI during first rise to maximum power. If one continued the irradiation, a diametral gap will be decreased due mainly to the fuel relocation and the swelling. Hence, higher the burn-up, smaller the rod diametral gap. This gap closure will tend to cause the greater PCMI.

Influence of burn-up on PCIOMR is studied by the fuel rod I-3 shown in Table 2. This was irradiated continuously in the course of PCIOMR-II experiments. Power history of this rod is shown in Fig. 11. As seen from the figure, this had PCIOMR (0.2 kW/mh) during first rise to maximum power and scrummed immediately after reaching 40 kW/m. At approximate burn-up of 1 GWd/tU , this had PCIOMR (0.4 kW/mh) repeatedly.

Result of our reassessment is shown in Figure 12. The followings are obtained :

(1) The magnitude of axial maximum strain at 1 GWd/tU denoted as $-\bullet-$ is smaller of order 40 % than that at start-up (denoted as $-\circ-$). At burn-up of 1 GWd/tU, the magnitudes of axial and diametral deformations become relatively smaller than at zero burn-up. There is nearly one to one correspondence between axial strain

and diametral one. Residual strain at this burn-up was almost zero. Thus, fuel deformed elastically.

(2) PCIOMR did not accompany the apparent relaxation.

Fuel behaviors before and after scrum were examined. The followings are obtained :

(1) Power rise rate was continued with 0.2 kW/mh from 30 kW/m to 40 kW/m. the experiment was then stopped due to coolant leakage at 40 kW/m. After repairment of coolant system, the experiment restarted. Power rise rate was 8 kW/mh. The magnitude of PCMI before and after scrum was compared with each other. Deformation shown in Fig. 12 is relatively different mainly because the former (denoted as $-\bigcirc-$) was affected much by fuel relocation than the latter. However, a magnitude of deformation of the two at 40 kW/m was almost the same. This might be due to disappearance of relocation effect at the power.

Ridge height at 1.0 GWd/tU was plotted as a function of hoop strain. It is shown in Fig. 13. For comparison, ridge height at start-up is included. Comparing with start-up, a magnitude of ridging and hoop strain at 1 GWd/tU was relatively small. Thus, initial PCIOMR is still effective to reduce PCMI at progressed burn-up.

4.2 PCIOMR at 14 GWd/tU

At burn-up of about 14 GWd/tU, a typical BWR type fuel rod having as-built gap by 0.10mm had slow power rise (0.2kW/mh). The power rise rate is similar to which carried out in PCIOMR-II experiment. Before this slow power rise, as shown in Fig. 14, the rod had several PCIOMR operations at various burn-up levels. Cladding outer diameter and axial strain were monitored continuously.

Result of reassessment for effectiveness of the last PCIOMR envelop is shown in Fig. 15. It is revealed from the figure that there is no significant effect of power rise rate on diametral and on axial PCMI. We found that PCIOMR operation at this case was not significant for reducing the PCMI. This might be due to the condition of fuel rod which was still within the previous PCIOMR envelopes.

5. CONCLUSION

From the reassessment of PCIOMR-I experiment, we obtained the followings:

(1) Fuel deformation during PCIOMR (0.2 kW/mh) was elastic but one during fast power rise (8 kW/mh) was plastic.

(2) A magnitude of deformation caused by PCIOMR was almost 50% small than one caused by fast power rise. PCIOMR is significantly influential to reducing the magnitude of PCMI

and diametral one. Residual strain at this burn-up was almost zero. Thus, fuel deformed elastically.

(2) PCIOMR did not accompany the apparent relaxation.

Fuel behaviors before and after scrum were examined. The followings are obtained :

(1) Power rise rate was continued with 0.2 kW/mh from 30 kW/m to 40 kW/m. the experiment was then stopped due to coolant leakage at 40 kW/m. After repairment of coolant system, the experiment restarted. Power rise rate was 8 kW/mh. The magnitude of PCMI before and after scrum was compared with each other. Deformation shown in Fig. 12 is relatively different mainly because the former (denoted as − ○ −) was affected much by fuel relocation than the latter. However, a magnitude of deformation of the two at 40 kW/m was almost the same. This might be due to disappearance of relocation effect at the power.

Ridge height at 1.0 GWd/tU was plotted as a function of hoop strain. It is shown in Fig. 13. For comparison, ridge height at start-up is included. Comparing with start-up, a magnitude of ridging and hoop strain at 1 GWd/tU was relatively small. Thus, initial PCIOMR is still effective to reduce PCMI at progressed burn-up.

4.2 PCIOMR at 14 GWd/tU

At burn-up of about 14 GWd/tU, a typical BWR type fuel rod having as-built gap by 0.10mm had slow power rise (0.2kW/mh). The power rise rate is similar to which carried out in PCIOMR-II experiment. Before this slow power rise, as shown in Fig. 14, the rod had several PCIOMR operations at various burn-up levels. Cladding outer diameter and axial strain were monitored continuously.

Result of reassessment for effectiveness of the last PCIOMR envelop is shown in Fig. 15. It is revealed from the figure that there is no significant effect of power rise rate on diametral and on axial PCMI. We found that PCIOMR operation at this case was not significant for reducing the PCMI. This might be due to the condition of fuel rod which was still within the previous PCIOMR envelopes.

5. CONCLUSION

From the reassessment of PCIOMR-I experiment, we obtained the followings:

(1) Fuel deformation during PCIOMR (0.2 kW/mh) was elastic but one during fast power rise (8 kW/mh) was plastic.

(2) A magnitude of deformation caused by PCIOMR was almost 50% small than one caused by fast power rise. PCIOMR is significantly influential to reducing the magnitude of PCMI

at ridging. The mechanism of this might be fuel creep, that is, relaxation.

(3) At BOL, the magnitude of integrated axial strain was not equal to that of average diametral strain in the same fuel rod. The former is about 60% greater than the latter. From the reassessment of PCIOMR-II experiment, we obtained the followings:

(4) At BOL, the fuel rod diametral gap by 0.21mm caused little PCMI. However, the fuel rod with diametral gap by 0.06mm caused greater PCMI. The magunitudes of PCMI along axial and diametral direction during PCIOMR were significaltly different. This was attributed to fuel densification stability in the used fuels.

(5) The magnitude of integrated axial strain was not equal to that of averaged diametral strain. PCIOMR is effective to reduce the magnitude of ridging at high power level.

(6) The magnitude of PCMI at burn-up of 1 GWd/tU becomes relatively small than that at BOL. The magnitude of PCMI between axial integrated strain and averaged diametral strain

ACKNOWLEDGMENT

Thanks are addressed to Drs. T. Fujishiro, Head of Reactivity Accident Laboratory, and J. Nakamura of Fuel Reliability Laboratory, Dep. Fuel Safety Research, JAERI for their encouragement and valuable comments. The authors wish to acknowledge the kind cooperation of the following Japanese and American vendors in allowing these data to be presented here. Hitachi Ltd, Toshiba Corporation and General Electric Company.

REFERENCES

(1) Y. Yukawa et al,: "Operating Experience of Hamaoka Nuclear Power Station", J. At. Energy Soc. Japan, 19 [6], 399 (1977) (in Japanese)

(2) Official open report for patent : 50-143999, (Nov. 19 1975) (in Japanese)

(3) R. Traccucci : "PCI in commercial PWRs", IAEA Specialists Meetings on Pellet Cladding Interaction for Water Reactors, Vienna, Austria (1977)

(4) C. B. Patterson et al,: "Measurements of the effects of power ramp rate on mechanical interaction at beginning of irradiation", paper presented at the Enlarged Halden Programme Group Meeting, Hanko, Norway (1979)

at ridging. The mechanism of this might be fuel creep, that is, relaxation.

(3) At BOL, the magnitude of integrated axial strain was not equal to that of average diametral strain in the same fuel rod. The former is about 60% greater than the latter. From the reassessment of PCIOMR-II experiment, we obtained the followings:

(4) At BOL, the fuel rod diametral gap by 0.21mm caused little PCMI. However, the fuel rod with diametral gap by 0.06mm caused greater PCMI. The magunitudes of PCMI along axial and diametral direction during PCIOMR were significatly different. This was attributed to fuel densification stability in the used fuels.

(5) The magnitude of integrated axial strain was not equal to that of averaged diametral strain. PCIOMR is effective to reduce the magnitude of ridging at high power level.

(6) The magnitude of PCMI at burn-up of 1 GWd/tU becomes relatively small than that at BOL. The magnitude of PCMI between axial integrated strain and averaged diametral strain

ACKNOWLEDGMENT

Thanks are addressed to Drs. T. Fujishiro, Head of Reactivity Accident Laboratory, and J. Nakamura of Fuel Reliability Laboratory, Dep. Fuel Safety Research, JAERI for their encouragement and valuable comments. The authors wish to acknowledge the kind cooperation of the following Japanese and American vendors in allowing these data to be presented here. Hitachi Ltd, Toshiba Corporation and General Electric Company.

REFERENCES

(1) Y. Yukawa et al,: "Operating Experience of Hamaoka Nuclear Power Station", J. At. Energy Soc. Japan, 19 [6], 399 (1977) (in Japanese)

(2) Official open report for patent : 50-143999, (Nov. 19 1975) (in Japanese)

(3) R. Traccucci : "PCI in commercial PWRs", IAEA Specialists Meetings on Pellet Cladding Interaction for Water Reactors, Vienna, Austria (1977)

(4) C. B. Patterson et al,: "Measurements of the effects of power ramp rate on mechanical interaction at beginning of irradiation", paper presented at the Enlarged Halden Programme Group Meeting, Hanko, Norway (1979)

at ridging. The mechanism of this might be fuel creep, that is, relaxation.

(3) At BOL, the magnitude of integrated axial strain was not equal to that of average diametral strain in the same fuel rod. The former is about 60% greater than the latter. From the reassessment of PCIOMR-II experiment, we obtained the followings:

(4) At BOL, the fuel rod diametral gap by 0.21mm caused little PCMI. However, the fuel rod with diametral gap by 0.06mm caused greater PCMI. The magunitudes of PCMI along axial and diametral direction during PCIOMR were significatly different. This was attributed to fuel densification stability in the used fuels.

(5) The magnitude of integrated axial strain was not equal to that of averaged diametral strain. PCIOMR is effective to reduce the magnitude of ridging at high power level.

(6) The magnitude of PCMI at burn-up of 1 GWd/tU becomes relatively small than that at BOL. The magnitude of PCMI between axial integrated strain and averaged diametral strain

ACKNOWLEDGMENT

Thanks are addressed to Drs. T. Fujishiro, Head of Reactivity Accident Laboratory, and J. Nakamura of Fuel Reliability Laboratory, Dep. Fuel Safety Research, JAERI for their encouragement and valuable comments. The authors wish to acknowledge the kind cooperation of the following Japanese and American vendors in allowing these data to be presented here. Hitachi Ltd, Toshiba Corporation and General Electric Company.

REFERENCES

(1) Y. Yukawa et al,: "Operating Experience of Hamaoka Nuclear Power Station", J. At. Energy Soc. Japan, 19 [6], 399 (1977) (in Japanese)

(2) Official open report for patent : 50-143999, (Nov. 19 1975) (in Japanese)

(3) R. Traccucci : "PCI in commercial PWRs", IAEA Specialists Meetings on Pellet Cladding Interaction for Water Reactors, Vienna, Austria (1977)

(4) C. B. Patterson et al,: "Measurements of the effects of power ramp rate on mechanical interaction at beginning of irradiation", paper presented at the Enlarged Halden Programme Group Meeting, Hanko, Norway (1979)

(5) T. Matsumoto et al,: "PCMI as a function of power ramp conditions (IFA-502 data analysis)", paper presented at the Enlarged Halden Programme Group Mtg. F2-2, Hanko, Norway (1981)

(6) T. Hosokawa et al,: "Data analysis for IFA-502 in HBWR", Annual meeting of the Atomic Energy Society of Japan, Tokyo Japan (1981)

(7) K. Yanagisawa : "An Evaluation of the Influence of Fuel Design Parameters and Burnup on Pellet/Cladding Interaction for Boiling Water Reactor Fuel Rod Through In-core Diameter Measurement", Nucl. Technol. 73, 36 (1986)

Table 1 Characteristics of fuel rods used in PCIOMR-I experiment[4]

Items	Slow power rise experiment (0.2 kW/mh)	Fast power rise experiment (8 kW/mh)
1. Fuel		
1.1 Material	Sintered UO_2 pellets	Sintered UO_2 pellets
1.2 Enrichment (% U-235)	9.88%	9.88%
1.3 Density	10.45 gm/cc	10.45 gm/cc
1.4 Pellet diameter	10.58 mm	10.58 mm
1.5 Pellet length	10.9 mm	10.9 mm
1.6 Dishing	None	None
1.7 Edge chamfer (mm)	0.36 x 0.36	0.36 x 0.36
2. Cladding		
2.1 Material	Zircaloy-2	Zircaloy-2
2.2 Heat treatment	Recrystallized	Recrystallized
2.3 Surface treatment	Autoclaved	Autoclaved
2.4 Clad O.D.	12.24 mm	12.24 mm
2.5 Clad I.D.	10.65 mm	10.65 mm
3. Assembly		
3.1 Total column length	395 mm	393 mm
3.2 Enriched fuel length	382 mm	383 mm
3.3 Enriched fuel weight	345 mm	346 mm
3.4 Diametral gap	0.075 mm	0.075 mm
3.5 Fill gas	He at 0.1MPa	He at 0.1MPa

Table 2 Characteristics of fuel rods used in PCIOMR-II experiment[5-6]

Series of Experiment	I			II			III			IV		
Rod	I-1	I-2	I-3*	II-1	II-2	I-3	III-1	III-2	I-3	IV-1	IV-2	I-3
Diametral gap (μm)	60	110	210	40	70	210	40	70	210	60	40	210
Fuel form	Sintered and ground UO_2 pellets											
Enrichment (w/o)	10.04	10.04	10.04	10.04	10.04	10.04	10.04	10.04	10.04	10.00	10.00	10.04
Density (Mg/m^3)	10.52	10.52	10.52	10.52	10.52	10.52	10.52	10.52	10.52	10.52	10.52	10.52
Pellet diameter (mm)	10.58	10.55	10.44	10.58	10.55	10.44	10.58	10.55	10.44	10.58	10.56	10.44
(L/D)	(0.95)	(0.96)	(0.97)	(0.95)	(0.96)	(0.97)	(0.95)	(0.96)	(0.97)	(0.95)	(0.96)	(0.97)
Edge chamfer (mm)	0.26x0.40	0.25x0.39	0.23x0.36	0.26x0.40	0.25x0.39	0.23x0.36	0.26x0.40	0.25x0.39	0.23x0.36	0.25x0.40	0.25x0.39	0.23x0.36
Cladding	Zircaloy-2											
Cladding state	Fully annealed: pickled, anodized and autoclaved											
cladding O.D. (mm)	12.273	12.268	12.28	12.245	12.240	12.28	12.24	12.24-26	12.28	12.24	12.24-26	12.28
cladding I.D. (mm)	10.64	10.66	10.65	10.62	10.62	10.65	10.62	10.62	10.65	10.62	10.62	10.65
Fuel length (mm)	341 active, 361 total, 102 hollow											
Plenum (ml)	7.7											
Filler gas	He 0.1 MPa											

* This was used continuously in the series of experiment

Table 3 Fuel deformation data at representative power level evaluated from in-core measurement in PCIOMR-I experiment: Ref.(4)

Ridge height and axial strain during slow power rise (0.2 kW/mh)					Ridge height and axial strain during fast power rise (8 kW/mh)				
Power (kW/m)	Dr(1) (%)	Dt(2) (%)	Power (kW/m)	ε_z(3) (%)	Power (kW/m)	Dr(1) (%)	Dt(2) (%)	Power (kW/m)	ε_z(3) (%)
7.6	0.0	0.0	5.0	0.0	2.7	0.0	0.0	5.0	0.0
16.3	-0.028	0.024	10.0	0.0	15.7	-0.003	0.056	10.0	0.028
16.9	-0.008	0.024	15.0	0.019	20.4	0.024	0.048	15.0	0.037
19.8	-0.020	0.032	20.0	0.036	24.8	0.048	0.053	20.0	0.057
22.5	0.008	0.039	25.0	0.050	29.3	0.010	0.070	25.0	0.097
26.6	0.016	0.039	30.0	0.064	32.5	0.105	0.094	30.0	0.119
28.3	0.033	0.048	35.0	0.070	35.5	0.146	0.127	35.0	0.159
31.4	0.049	0.064	40.0	0.080	39.1	0.162	0.143	40.0	0.193
33.9	0.057	0.073	43.0	0.084	40.1	0.179	0.167	42.0	0.193
35.8	0.065	0.078	0.0	0.0	42.5	0.187	0.186	0.0	0.065
37.9	0.065	0.078			42.1	0.170	0.151		
39.8	0.073	0.098			41.9	0.162	0.151		
41.6	0.090	0.106			39.1	0.113	0.108		
44.8	0.098	0.122			36.3	0.073	0.091		
40.1	0.033	0.098			33.4	0.089	0.096		
35.8	0.033	0.090			29.3	0.073	0.091		
30.2	0.033	0.092			24.3	0.064	0.087		
26.2	0.024	0.030			2.7	0.032	0.050		
2.6	0.008	0.015			1.7	0.024	0.0		

Note: (1) Dr : Average rod outer diameter at pellet-to-pellet interface location

(2) Dt : Average rod outer diameter at mid-pellet location

(3) ε_z: Integrated rod axial elongation

Table 4 Fuel deformation data at representative power level evaluated from in-core measurement in PCIOMR-II experiment: Ref.(5-6)

Experiment I Fresh fuel, 0.06mm gap Ramp rate=0.7 kW/mh			Experiment II Fresh fuel, 0.04mm gap Ramp rate=0.2 kW/mh			Experiment III[3] Fresh fuel, 0.04mm gap Ramp rate=282 kW/mh			Experiment IV Fresh fuel, 0.06mm gap Ramp rate = 0.197 kW/mh			Preirradiated fuel[4], 0.06mm gap Ramp rate = 0.36 kW/mh Burnup = 1.0 GWd/tU		
Power (kW/m)	Dr[1] (%)	ε_z[2] (%)	Power (kW/m)	Dr (%)	ε_z (%)	Power (kW/m)	Dr (%)	ε_z (%)	Power (kW/m)	Dr (%)	ε_z (%)	Power (kW/m)	Dr (%)	ε_z (%)
5	0.0	0.003	5	0.010	0.018	5	0.01	0.023	5	0.028	0.028	5	0.007	0.002
10	0.0	0.010	10	0.035	0.053	10	0.02	0.067	10	0.048	0.058	10	0.013	0.005
15	0.004	0.023	15	0.054	0.097	15	0.05	0.109	15	0.086	0.103	15	0.022	0.010
20	0.020	0.053	20	0.078	0.140	20	0.08	0.138	20	0.102	0.164	20	0.030	0.015
25	0.038	0.088	25	0.106	0.180	25	0.04	0.123	25	0.124	0.200	25	0.030	0.026
30	0.049	0.116	28	0.120	0.208	Medium (4.3kW/mh) to			26	0.136	0.230	30	0.030	0.030
Slow ramp			Slow ramp			fast ramp (282kW/mh)			Slow ramp (8kW/mh→0.2kW/mh)			Slow ramp (8kW/mh→0.36kW/mh)		
(8kW/mh → 0.7kW/mh)			(8kW/mh → 0.2kW/mh)			67	0.41	0.33	27	0.136	0.230	32	0.030	0.030
32	0.047	0.094	30	0.120	0.191	4	0.28	0.15	30	0.154	0.200	34	0.030	0.035
34	0.060	0.081	32	0.130	0.147				32	0.159	0.185	36	0.046	0.040
36	0.076	0.073	34	0.136	0.136				34	0.174	0.178	38	0.050	0.045
38	0.092	0.065	36	0.140	0.132				36	0.170	0.175	40	0.055	0.035
40	0.110	0.059	38	0.142	0.132				38	0.166	0.170	42	0.068	0.064
42	0.120	0.059	40	0.146	0.132				40	0.180	0.168	44	0.065	0.073
44	0.134	0.059	42	0.150	0.132				Reactor scrum			46	0.075	0.078
46	0.144	0.059	44	0.154	0.132				Re-ramp with 8kW/mh			48	0.082	0.078
27	0.052	0.015	46	0.162	0.132				0	0.048	0.088	0	0.01	0.00
0.8	0.0	0.0	28	0.133	0.117				5	0.052	0.095			
			3.3	0.004	0.009				10	0.058	0.097			
									15	0.065	0.100			
									20	0.074	0.102			
									25	0.090	0.105			
									30	0.110	0.115			
									35	0.135	0.155			
									40	0.180	0.175			
									Slow ramp (8kW/mh→0.2kW/mh)					
									42	0.195	0.168			
									44	0.203	0.165			
									2	0.140	0.088			

Note: (1) Dr : Average rod outer diameter at pellet-to-pellet interface location
(2) ε_z: Integrated rod axial elongation
(3) Reference only in this report
(4) Slow power rise experiment at burn-up of 1 GWd/tU

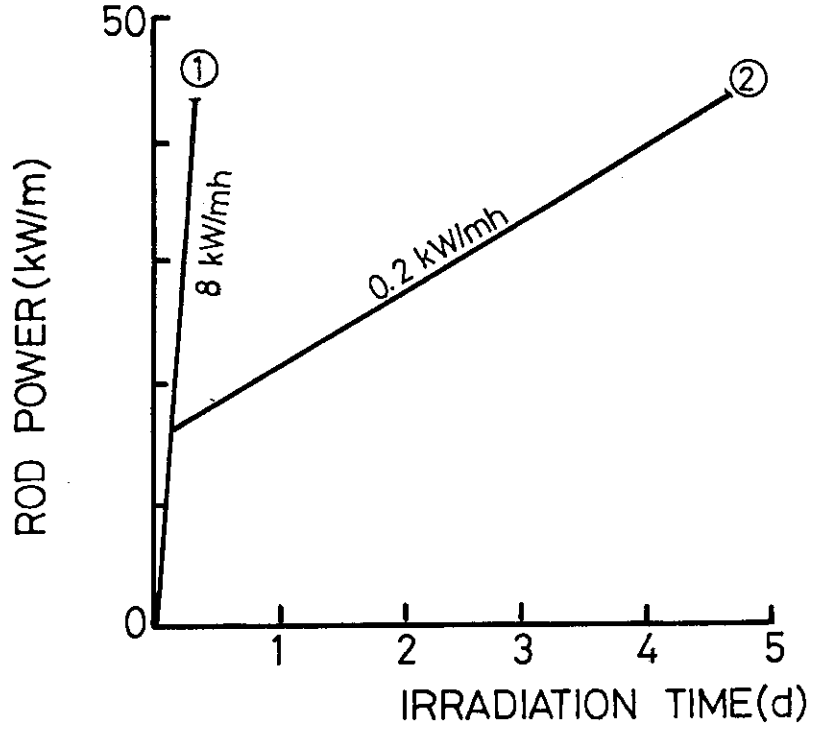

Fig. 1 Schematic representation of power rise rate used in the experiment[4]

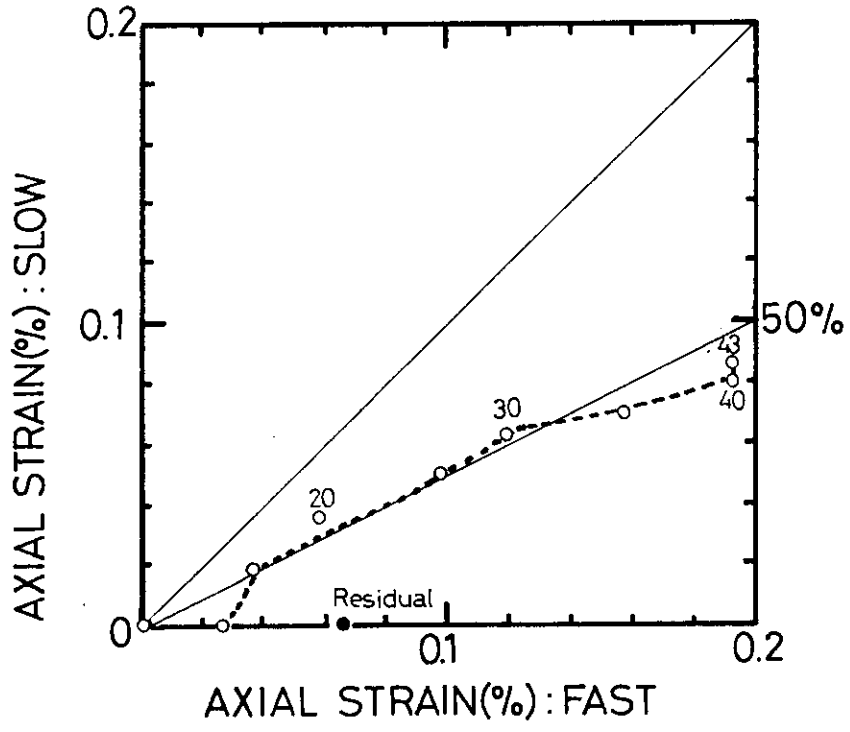

Fig. 2 Axial strain of 8×8 BWR type fuel rod under slow ramp (0.2 kW/mh) and that of 8×8 BWR type fuel rod under fast ramp (8 kW/mh), at representative power levels (Data given by open circles). Residual strain (full circle) after power removal is also shown.

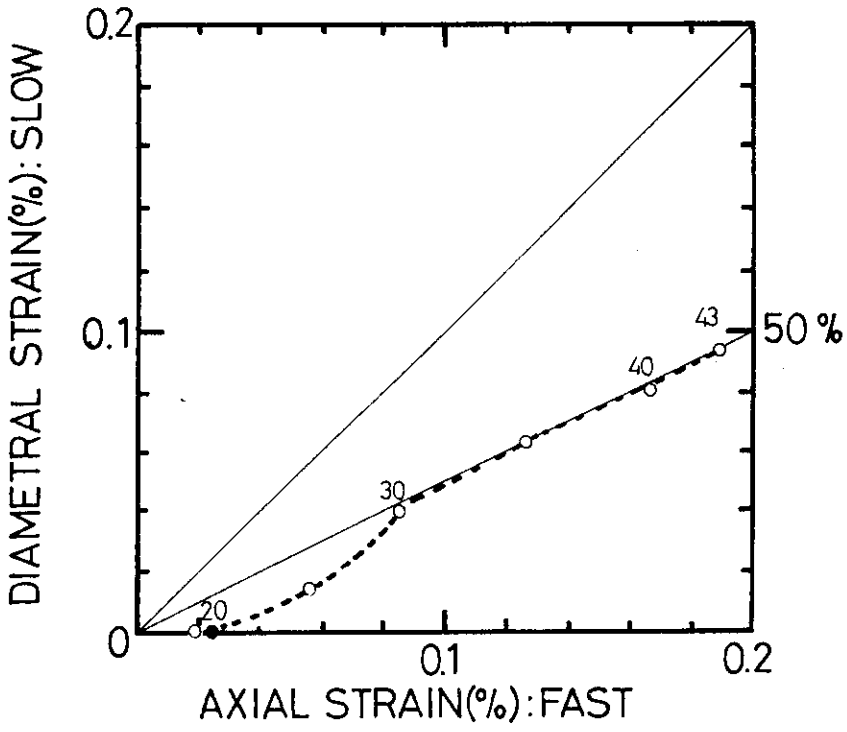

Fig. 3 Diametral strain of 8×8 BWR type fuel rod under slow power ramp (0.2 kW/mh) and axial strain of 8×8 BWR type fuel rod under fast ramp (8 kW/mh) at representative power levels (Data given by open circles). Residual strain after power removal is shown by full circle.

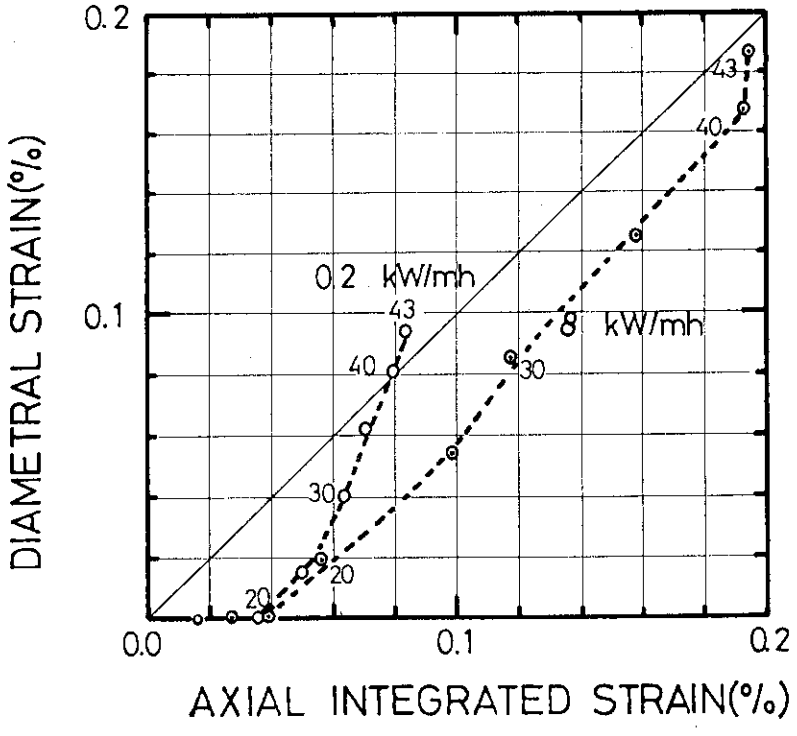

Fig. 4 Diametral strain of 8×8 BWR type fuel rod vs axial integrated strain as a function of power rise rate: Data were plotted at representative power levels.

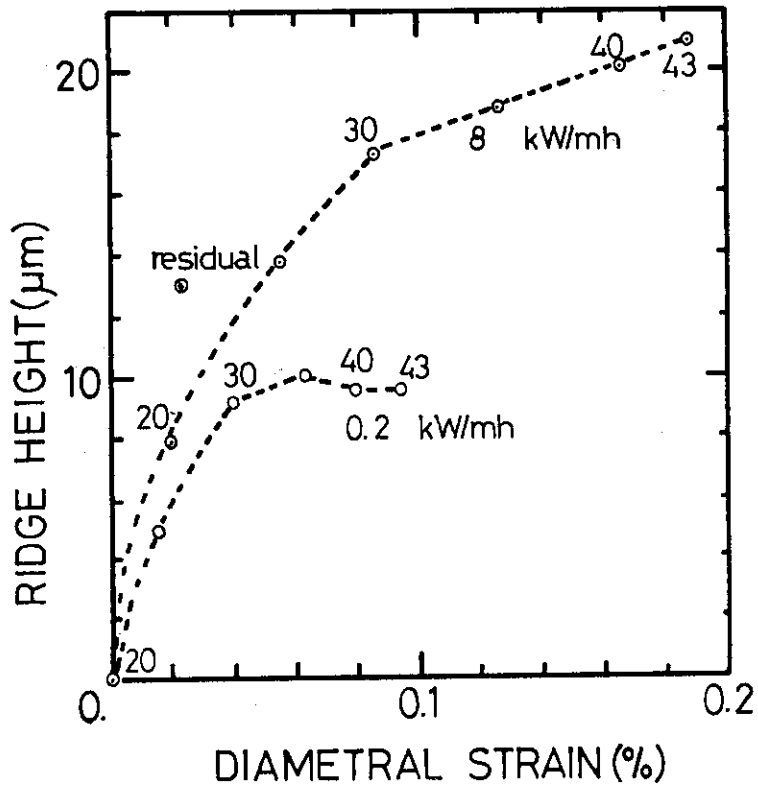

Fig. 5 Ridge heiqut vs diametral strain as a function of power rise rate: Data was plotted at representative power levels. "Residual" in the figure means data point of 8 kW/mh after power removal.

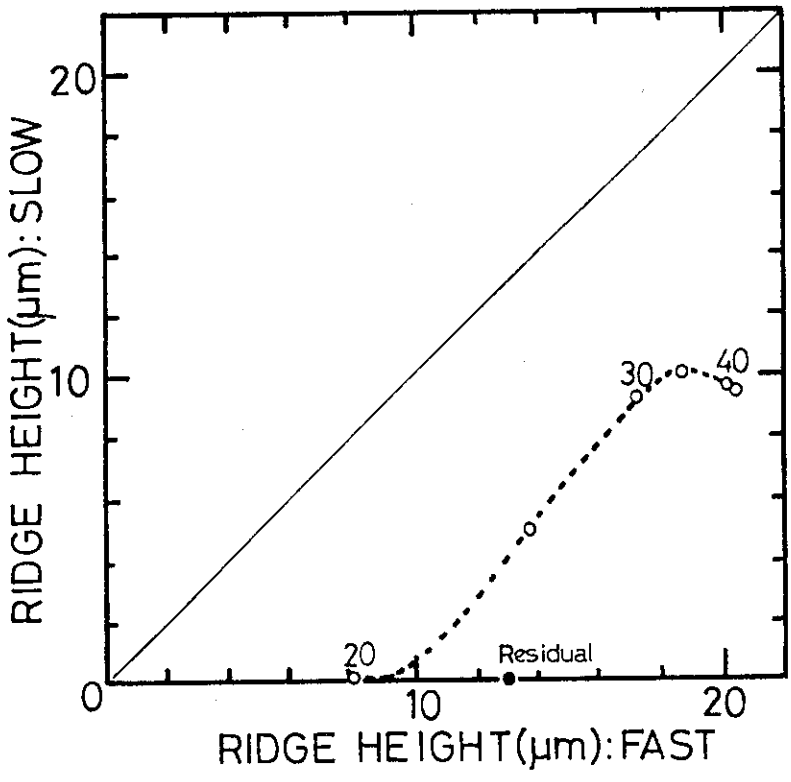

Fig. 6 Ridge height of 8×8 BWR type fuel rod under slow ramp (0.2 kW/mh) and that of 8×8 BWR type fuel rod under fast ranp (8 kW/mh), plotted by open circles. Residual ridge height after power removal is given by full circle.

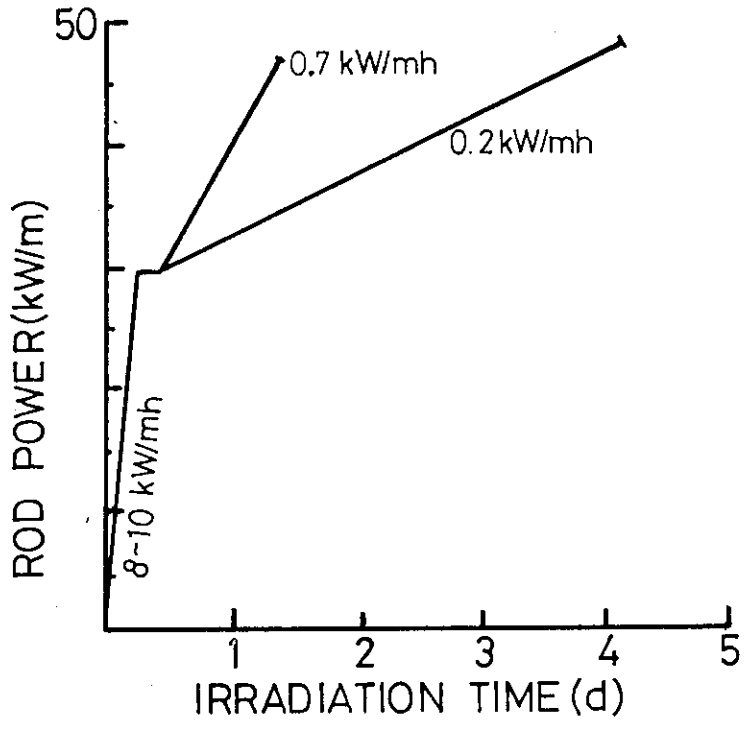

Fig. 7 Schematic representation of power rise rate used in the experiment[5], where PCIOMR started from power level of 30 kW/mh, followed by fast ramp by 8∿10 kW/m.

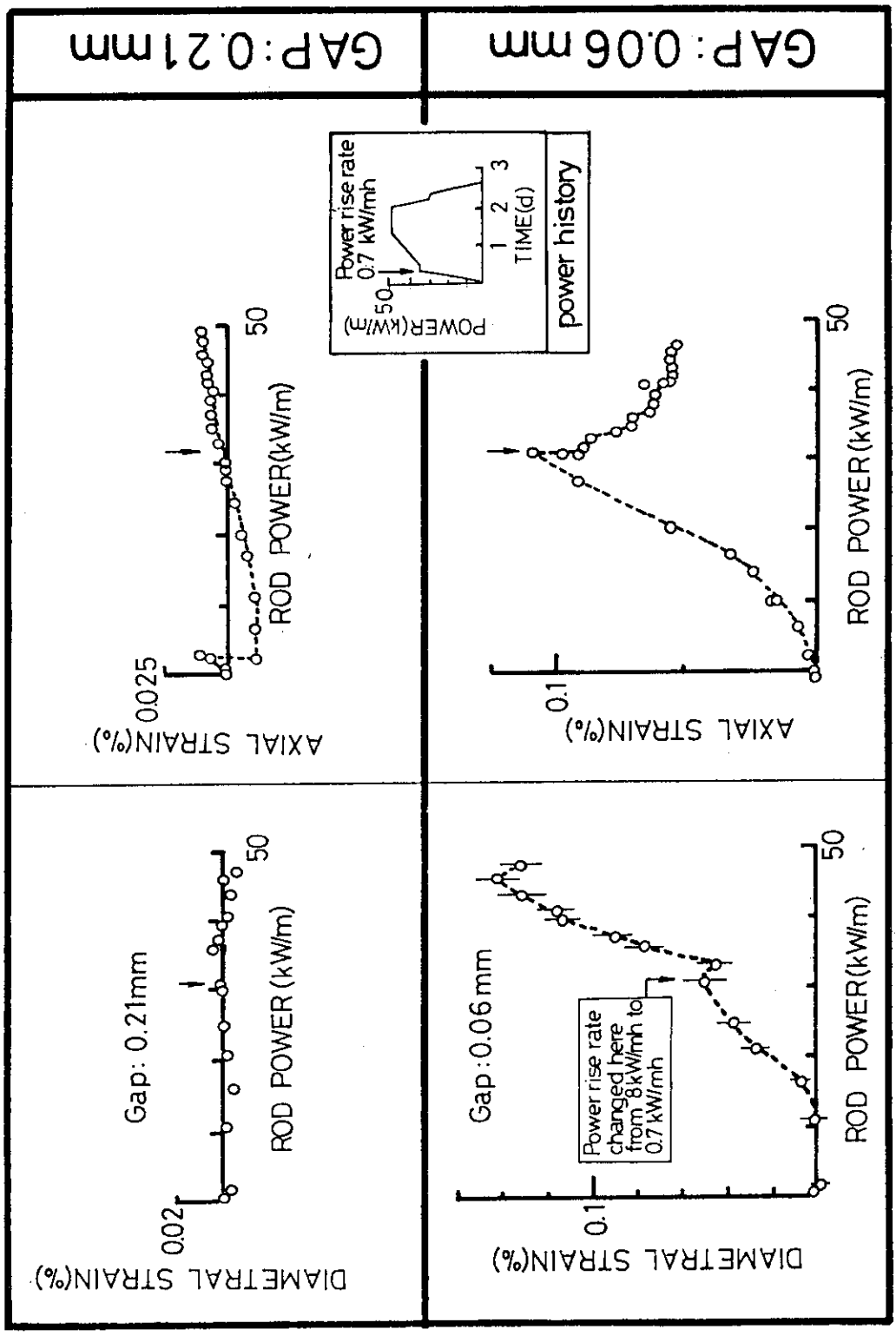

Fig. 8 Diametral and axial strains in two different gap rods, where power rise rate changed from 8 kW/mh to 0.7 kW/mh at arrow shown in the figure.

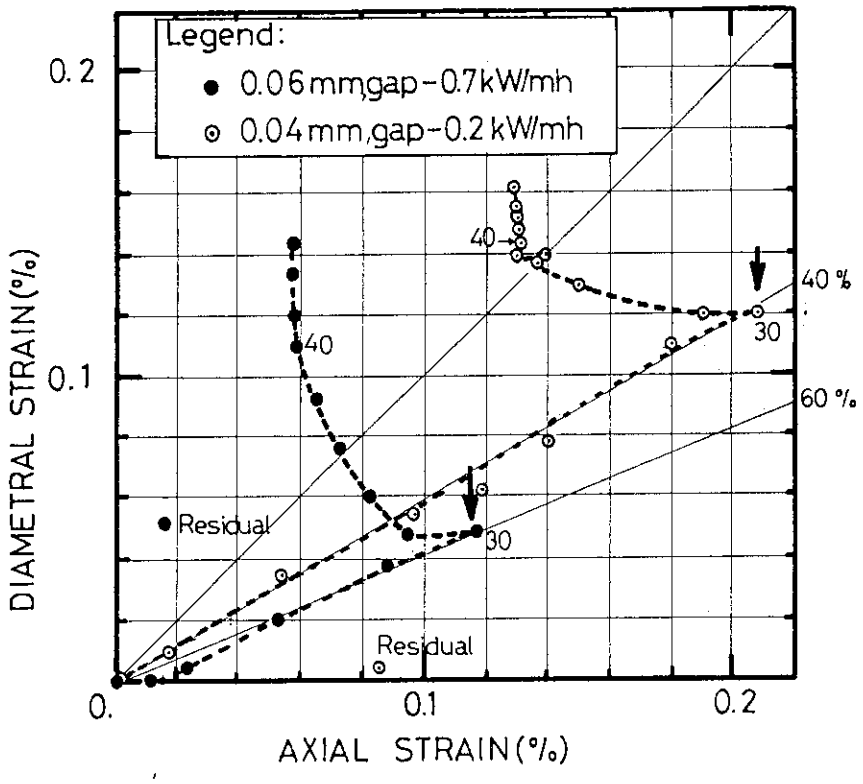

Fig. 9 Diametral strain of smaller gap rods vs axial strain as a function of power rise rate, where power rise rate was changed at location shown by arrow: Data was plotted at representative power levels, including residual strain after power removal.

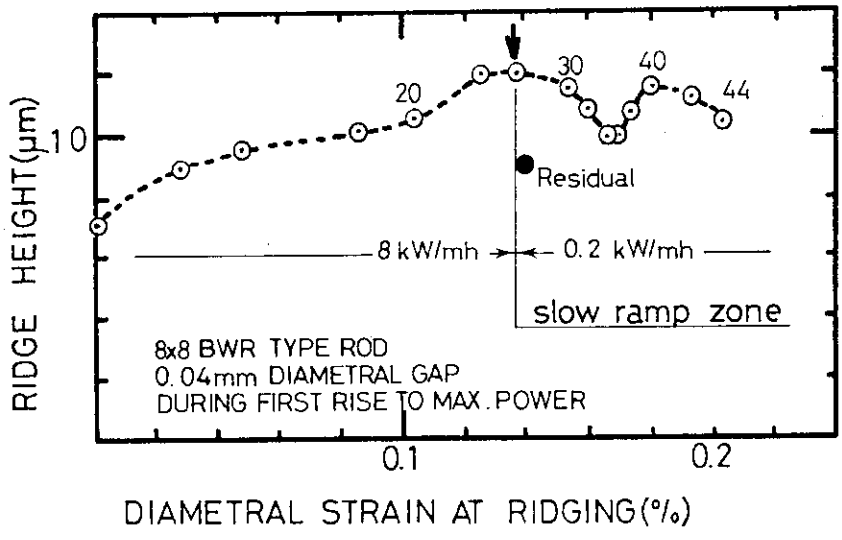

Fig. 10 Ridge height of 8×8 BWR fuel rod vs diametral strain at ridging as a function of power rise rate; where arrow is showing the location of power rise rate alternation and full mark is showing the residual ridge height after power removal.

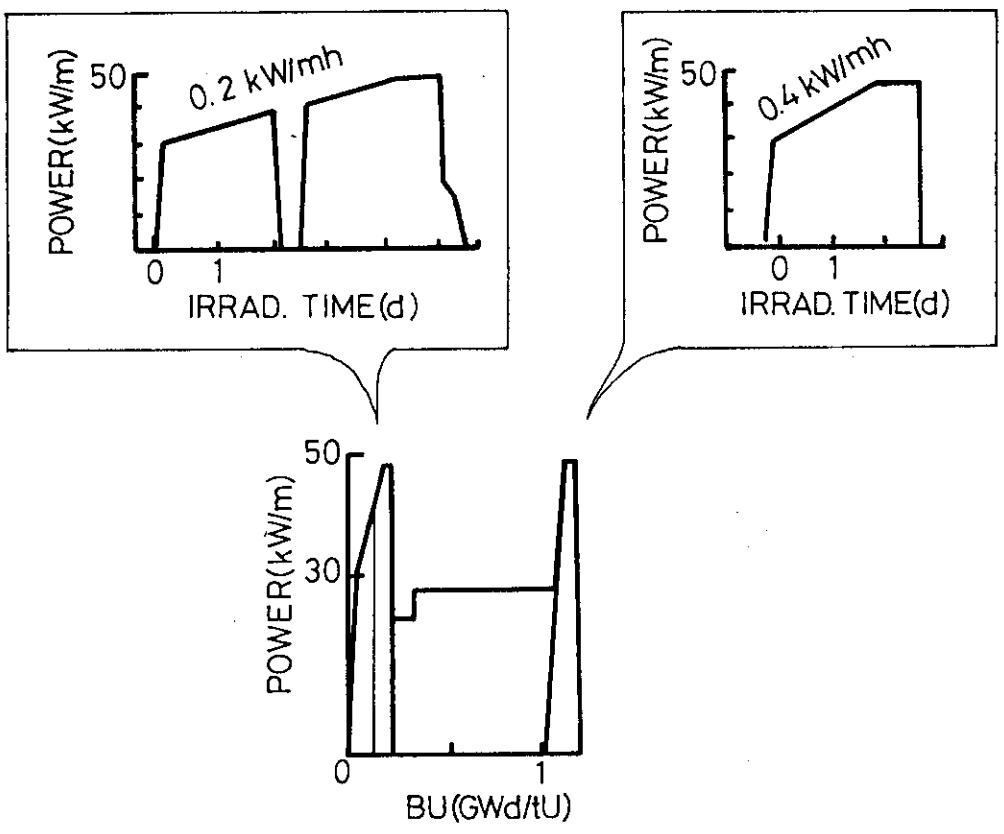

Fig. 11 Schematic representation of power history for PCIOMR (0.2 kW/mh) at beginning-of-life and for PCIOMR (0.4 kW/mh) at burn-up of 1 GWd/tU. Top two are magnification of each experiment.

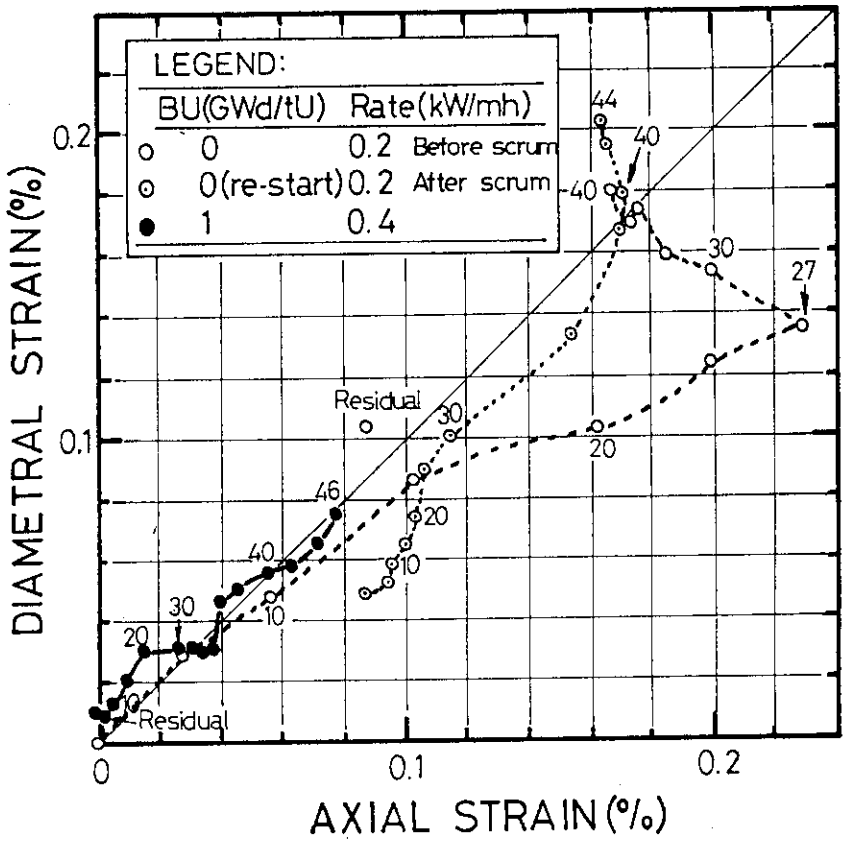

Fig. 12 Diametral strain of 8×8 BWR type fuel rod vs axial strain at different three experiments in which -○- mark shows first power rise to 40 kW/m, -⊙- mark shows second power rise to 44 kW/m after occurrence of scrum, and -●- mark shows power rise to 46 kW/m at burn-up of 1 GWd/t. Arrows indicate the location of power ramp rate alternation. Residual strain in each experiment except after scrum is also shown.

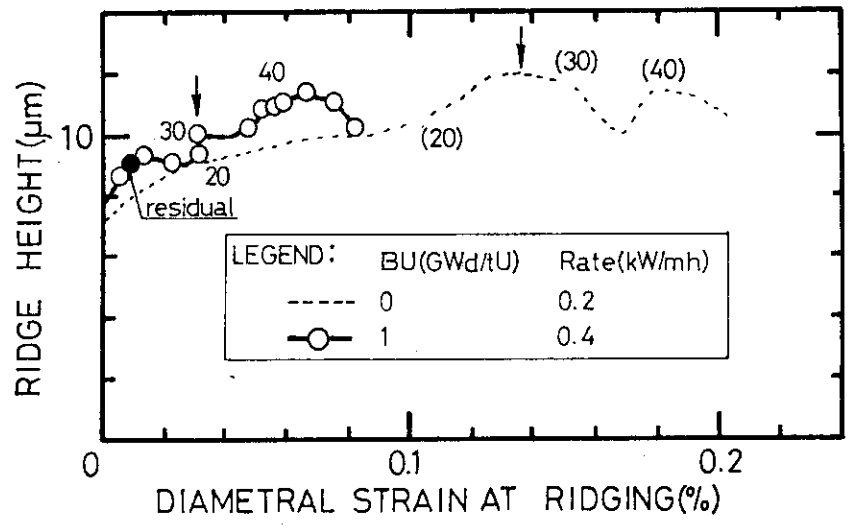

Fig. 13 Ridge height of 8×8 BWR type fuel rod vs diarmetral strain at ridging in which solid line is the data of 1 GWd/tU and dotted line is the data of first rise to maximum power; two arrows show the location of power rise rate change from 8 kW/mh to 0.2-0.4 kW/mh and －●－ mark shows residual strain of experiment at 1 GWd/tU.

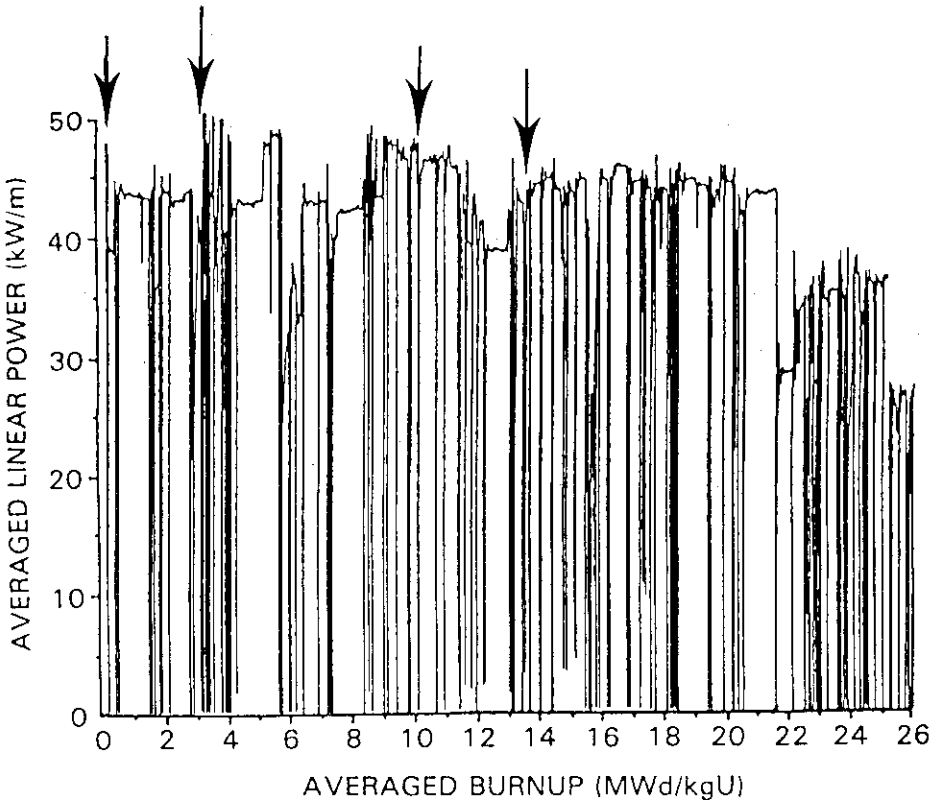

Fig. 14 Power history of BWR type fuel which had several PCIOMR operations (shown by arrows) during irradiation.

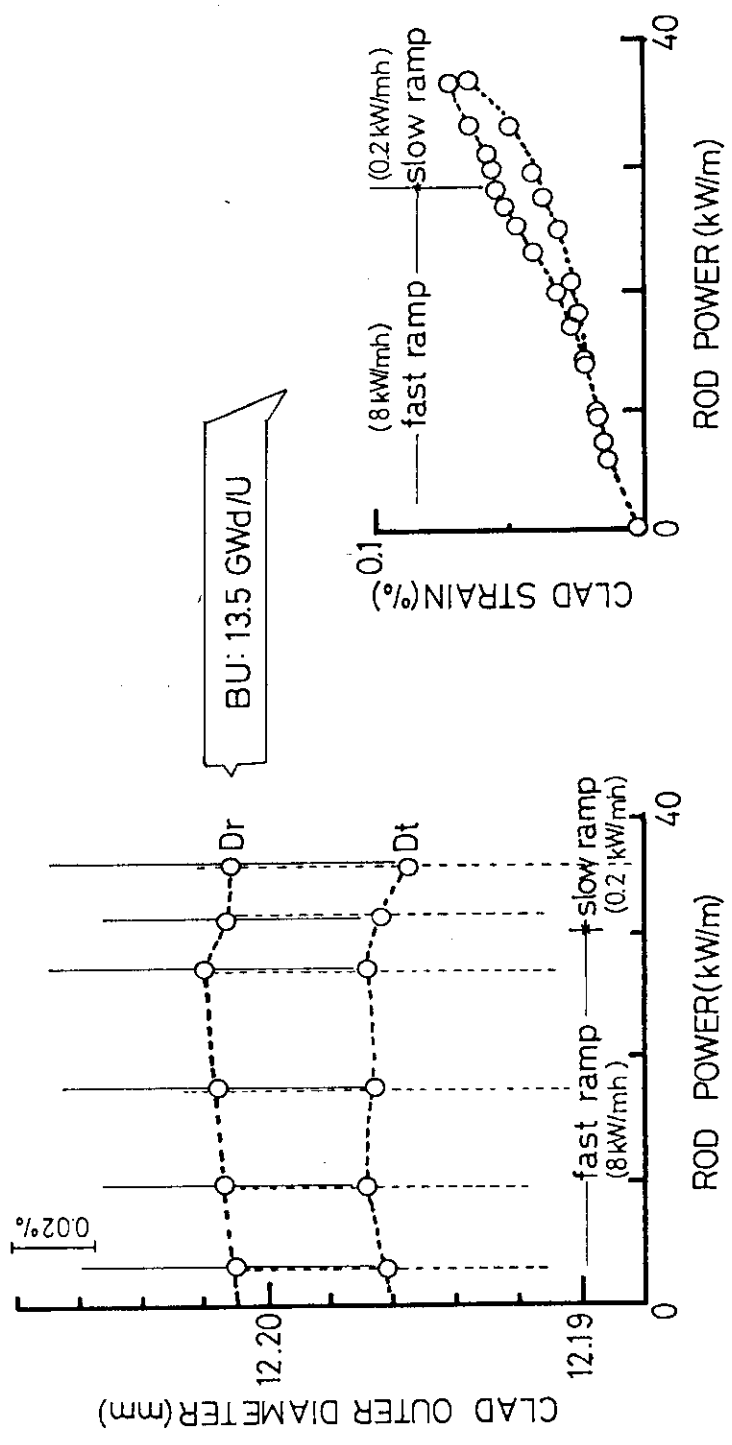

Fig. 15 (Left) Clad outer diameter at pellet-to-pellet interface (shown by Dr) and at mid-pellet location (shown by Dt) vs rod power and (Right) Clad axial strain vs rod power at burn-up of 13.5 GWd/tU; Fuel rod used here was typical BWR having initial diametral gap of 0.1 mm[7].